Asian Journal of Nanoscience and Materials, 2018, 1(1), 36-46.

FULL PAPER

Facile Green Synthesis of Fluorescent Carbon Quantum Dots from Citrus Lemon Juice for Live Cell Imaging

Aschalew Tadesse[a,b], Dharmasoth RamaDevi[d], MebrahtuHagos[a,c], GangaRao Battu[d], Keloth Basavaiah [a,*]

[a]*Department of Inorganic and Analytical chemistry, Andhra University, Visakhapatnam-530003, India.*
[b]*Department of Applied Chemistry, Adama Science and Technology University, 1888, Ethiopia.*
[c]*Faculty of Natural and Computational Sciences, Woldia University, 400, Ethiopia.*
[d]*AU College of Pharmaceutical Science, Andhra University, Visakhapatnam-530003, India.*

Received: 29 January 2018, Revised: 05 March 2018 and Accepted: 006 March 2018.

ABSTRACT: Facile and green one pot hydrothermal method was used for synthesis of fluorescent carbon quantum dots (CQDs) using citrus lemon juice as precursor. The synthesized CQDs were characterized using UV–Vis spectrophotometer, fluorescence spectrometer, transmission electron microscopy (TEM), X-ray diffraction (XRD), Fourier transform infrared spectrometer (FTIR), field emission scanning electron microscope equiped with energy dispersive X-ray spectroscopy (FESEM-EDS) and fluorescence microscopy. The obtained CQDs have high photoluminescence of 10.20% quantum yield. The photoluminescence intensity of CQDs depends on pH of the solution and maximum intensity obtained at pH of 6. The particle size of the carbon dots were distributed in narrow range of 2–10 nm with an average of 5.8 nm. The highly water soluble CQDs have high cell viability even at high concentration which rich up to 85%. MTT assay was used to investigate the potential application of CQDs and the results indicated that the material can be used as florescent probe in the cell imaging.

KEYWORDS: carbon quantum dots, citrus lemon juice, fluorescent, hydrothermal method, cell imaging.

GRAPPHICAL ABSTACT:

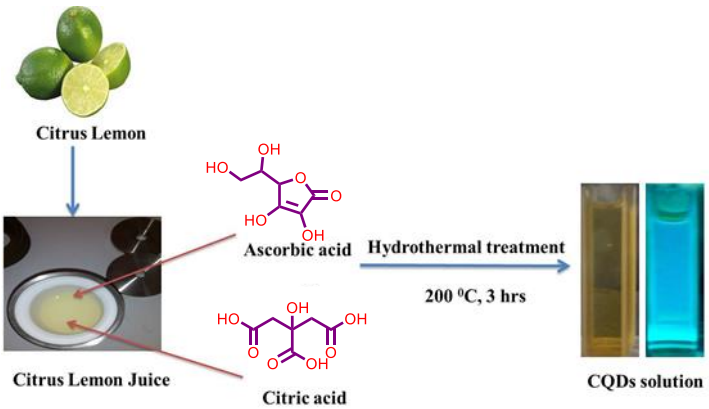

Introduction

Since the first discovery in 2004 [1] and designed synthesis in 2006 [2], carbon quantum dots (CQDs) have attracted a great deal of attention from the researchers due to their unique properties such as, low cost and

Asian Journal of Nanoscience and Materials

facile synthesis, chemical stability, high photoluminescence, and non-toxicity. The interesting property that gives popularity to CQDs is the highly stable, photobleaching resistant multicolour photoluminescence [3]. Moreover, the surface of the CQDs is rich with carboxylic acid functional groups which make them highly water soluble and suitable for functionalization with other functional groups for desired purposes [4,5], especially for biological applications. In relative to semiconductor quantum dots which are susceptible to toxic heavy metal leaching, CQDs have low toxicity and biocompatible for biological cell imaging and sensing [6,7]. Various cytotoxicity assay studies confirmed that CQDs are nontoxic to cells at concentration levels much higher than those commonly used for fluorescence labeling and imaging purposes [8-11]. In addition to the biocompatibility, CQDs are interesting fluorescent nanomaterials to biological labeling and imaging of cells due to its multicolour bright photoluminescence which can give bright alternative images of cells [12]. Therefore, study of synthesis and finding new cheap precursor for these important materials is very crucial. The two general methods for syntheses of CQDs are top-down and bottom-up methods [13]. Numerous methods such as electrochemical oxidation processes [14], arc discharge [1], hydrothermal cutting strategies [10], chemical oxidation methods [15], combustion/ thermal, and so on have been demonstrated for synthesis of CQDs. Some of the methods above required high costs, tedious steps, or special equipment. Hydrothermal method is a facile, one-step process with low synthesis cost when compared to other method and hence frequently used by researchers. In hydrothermal method, carbonization takes place at low temperature with self-created pressure and there is no any reaction product released to the environment and hence it is green method. Natural products and waste materials like orange juice, coriander leaves and orange waste peels have been used as carbon sources to prepare photoluminescent CQDs [16-18]. Exploration of new carbon sources for environmental friendly and economical synthesis of such photoluminescent CQDs is meaningful and desirable. In search of natural or less harmful chemicals as a precursor, the use of environmentally green, and low cost natural products are becoming the most promising for synthesis of the CQDs.

Citric acid is an excellent precursor to synthesize the CQDs due to its low carbonization temperature [19,20]. It is well known that the sour test of lemon juice is due to presence of acids of which the major is citric acid. Inspiring by these, we prepared highly fluorescent water soluble carbon quantum dots (CQDs) using lemon juice as precursor via eco-friendly green hydrothermal synthesis method. The as synthesized CQDs were characterized by TEM, FESEM-EDS, XRD, FTIR, UV-Vis spectrophotometer, and Fluorescence spectrometer and investigated for live cell imaging.

2 - Experimental

2.1 - Materials and Chemicals

Fresh lemon fruits were purchased from the local store nearby Andhra University and CQDs were synthesized from lemon juice via the hydrothermal process. Quinine sulfate dehydrate was procured from Loba Chemia Pvt. Ltd, Mumbai, India. Sulfuric acid was procured from Merck Life Science Pvt. Ltd, Mumbai, India. 100 mL stainless steel Teflon lined autoclave was used for hydrothermal synthesis. Milli-Q water was used throughout the experiment.

2.2 - Synthesis of Carbon Quantum Dots

Asian Journal of Nanoscience and Materials

A single step hydrothermal synthetic method was used to prepare carbon quantum dots (CQDs) using lemon juice as carbon source. In a typical procedure, 20 ml of filtered lemon juice was taken in a 100 mL Teflon-lined stainless steel autoclave and placed at 200 ^{0}C in muffle furnace for 3 h. After cooling down to room temperature, the as obtained black paste was dissolved in 15 mL of water and centrifuged at 3000 RPM for 15 min to remove insoluble matter. Dichloromethane was added to the brown solution formed and centrifuged at 3000 RPM for 20 min to remove unreacted organic moieties. The aqueous layer was separated from lower organic layer and centrifuged at 12000 RPM for 20 min three times to remove larger size particles and the brown yellowish supernatant were finally obtained. To further get the smaller particle size of CQDs, cleaning was done using column chromatographic separation in help of silica gel and dichloromethane as solvent. The resulting CQDs solution was kept in refrigerator at 4 ^{0}C for characterization and used for application. A series of CQDs were prepared with different reactants concentration, temperature or time via the same procedure in the expanded experiments to optimize the synthesis method using lemon juice as carbon source.

2.3 - Characterization

The morphology and microstructures of the synthesized CQDs were analyzed using transmission electron microscopy (TEM) and high resolution transmission electron microscopy (HRTEM, Jeol/JEM 2100, LaB6) operated at 200 kV. Fourier transform infrared spectra (FTIR) were obtained over the range of 400–4,000 cm^{-1} using a SHIMADZU-IR PRESTIGE-2 Spectrometer. Fluorescence properties of the samples were measured with Fluoromax-4 spectrofluorometer (HORIBA Scientific). Further morphology and composition of the CQDs were characterized using field emission scanning electron microscopy (FESEM, Zeiss Ultra-60) equipped with X-ray energy dispersive spectroscopy (EDS). UV–Vis absorption spectra were obtained using a UNICAM UV 500 (Thermo Electron Corporation). X-ray powder diffraction (XRD) pattern were recorded using PANalytical X'pert pro diffractometer using Cu-kα_1 radiation (45kV, 1.54056 Å; scan rate of 0.02 degree/sec).

2.4 - Quantum Yield

Quantum yield was calculated using the equation (eq. 1) using quinine sulphate in 0.1N sulphuric acid (the quantum yield of 54% at 365 nm) as a reference [23,24]. The UV–Vis absorption at 365nm and PL emission spectra (excited at 365 nm) of CQDs and reference were measured, respectively. The following equation used to calculate the QY:

$$QY_{Samp} = QY_{ref} \frac{I_{sam} A_{ref} n_{sam}^{\ 2}}{I_{ref} A_{sam} n_{ref}^{\ 2}} \quad \textbf{(1)}$$

where QY_{sam} and QY_{ref} are quantum yield of CQDs and reference respectively, I_{sam} and I_{ref} are emission intensity, A_{sam} and A_{ref} are UV–Vis absorbance, n_{sam} and n_{ref} are refractive index of sample and reference.

2.5 - Cytotoxicity Test

In vitro cytotoxicity of CQDs were evaluated on human breast adenocarcinoma (MCF7) cells by using the MTT assay. Cellular toxicity was determined by measuring the activity of mitochondrial enzymes in live cells to transform the soluble yellow MTT solution to an insoluble purple formazan product. The cells were cultured in 96-well tissue culture plates at a density of 1×10^4 cells per well. After adhering, the cells were incubated with a medium containing different doses of CQDs for 24 h. Subsequently, after incubation the medium

from each well was removed and the cells were washed in phosphate buffered solution (PBS). A fresh medium containing 10 µL of 0.5 mg mL^{-1} solution of MTT was added to each well and incubated for 4 h and then the medium was replaced with 150 µL of DMSO followed by shaking for 15 min to dissolve the formazan crystals. The absorbance of each well was recorded at 570 nm using a multimode microplate reader (Biotek, Cytation3). The untreated cells were used as controls for calculating the relative percentage cell viability from the following equation:

% Cell viability = (A_{570} in treated sample / A_{570} in control sample) × 100% (2)

2.6 - Multicolour Cell Imaging

Bioimaging potential of CQDs was tested using MCF7 Cells. MCF7 cells were seeded in 6-well culture plates at a density of 10^5 cells per well in DMEM containing 10 % Fetal bovine serum (FBS) and incubated for 24 h at 37 ^{0}C and 5 % CO_2. Then the medium was replaced with a fresh medium containing 0.025 mg/mL carbon quantum dots and further incubated for 6 h. After that the cells were washed thrice with PBS to remove extracellular CQDs, fixed with 4% paraformaldehyde and mounted using 50 % glycerol. Fluorescent images were recorded using "Zeiss LSM 510 Meta confocal Microscopy" at laser excitations of 405, 488 and 561 nm.

Results and Discussion

In this paper, green facile hydrothermal synthesis of CQDs using lemon juice as carbon precursor is presented. The morphological and structural properties of as prepared CQDs were confirmed by using TEM and HRTEM (Fig 1a and b). As seen from the results, the CQDs are quasi spherical nanoparticles with narrow size distribution. As calculated from TEM image using ImageJ software the particle size of the as prepared CQDs are distributed in diameter range of 2 – 10 nm with an average of 5.8 nm based on statistical analysis of more than 90 dots (histogram in Fig 1d). Fig 1c shows the selected area electron diffraction (SAED), the holes indicating the particle formation and the graphitic amorphous nature of the CQDs [13]. EDS (Fig 1e) result confirmed that the elemental compositions of the synthesised CQDs were only carbon and oxygen.

To evaluate the optical properties of the synthesised CQDs, UV–Vis absorption and fluorescence excitation and emission spectra were measured. The synthesized CQDs have two absorption peaks at 240 and 350 nm (Fig **2**, black line), which are probably assigned to the typical absorption of aromatic π – π* systems and the n – π* transition of CQDs respectively [25]. The brown yellowish aqueous solution of CQDs appears brilliant blue under UV irradiation (inset in Fig 2a and b) confirming the bright photoluminescence of the prepared CQDs. To describe the photoluminescence of CQDs, excitation and emission spectra were recorded usingspectrofluorometer and maximum excitation intensity obtained at wavelength of 365 nm (Fig 2, red line) while maximum emission intensity obtained at wavelength of 450 nm (Fig 2, blue line).

To address whether the synthesized CQDs showed excitation dependent photoluminescence or not, different emission spectra upon varying excitation wavelengths were recorded. Fig 3a demonstrates the photoluminescence emission spectra of the CQDs with excitation wavelengths from 300 nm to 420 nm. The sample reveals a strong fluorescence with the symmetrical emission peaks and as excitation wavelength increased

Asian Journal of Nanoscience and Materials

from 300 nm to 360 nm, the emission intensity increased and further change of the excitation wavelength from 360 nm to 420 nm resulted in regular decrease of emission intensity. Maximum emission intensity obtained at 360 nm excitation wavelength and changing excitation wavelength has no significant effect on emission wavelength. In addition to the strong down conversion photoluminescence properties, the synthesized CQDs show a clear up conversion photoluminescence feature. Fig 3b shows the photoluminescence spectra of CQDs excited by long wavelength light (600 nm to 800 nm) with the up converted emissions centered on emission wavelength of 450 nm, which is similar as the down conversion photoluminescence peaks. The quantum yield of the CQDs was about 10.20% by using quinine sulfate as reference. Fig 3c shows the 3D FL emission spectra of the CQDs with various excitation wavelengths from 300 nm to 400 nm in 4 nm increments. Fig 3d is excitation and emission contour map of CQDs which indicate multicolour photoluminescence properties. The photoexcitation of carbon quantum dots is due to π-plasmon absorption in the core carbon nanoparticles [26]. In addition, the FL properties of CQDs are significantly affected by the surface chemistry of the particles [27]. The average FWHM obtained from the fluorescence emission was 82 nm which confirm narrow size distribution of the prepared CQDs [19,28].

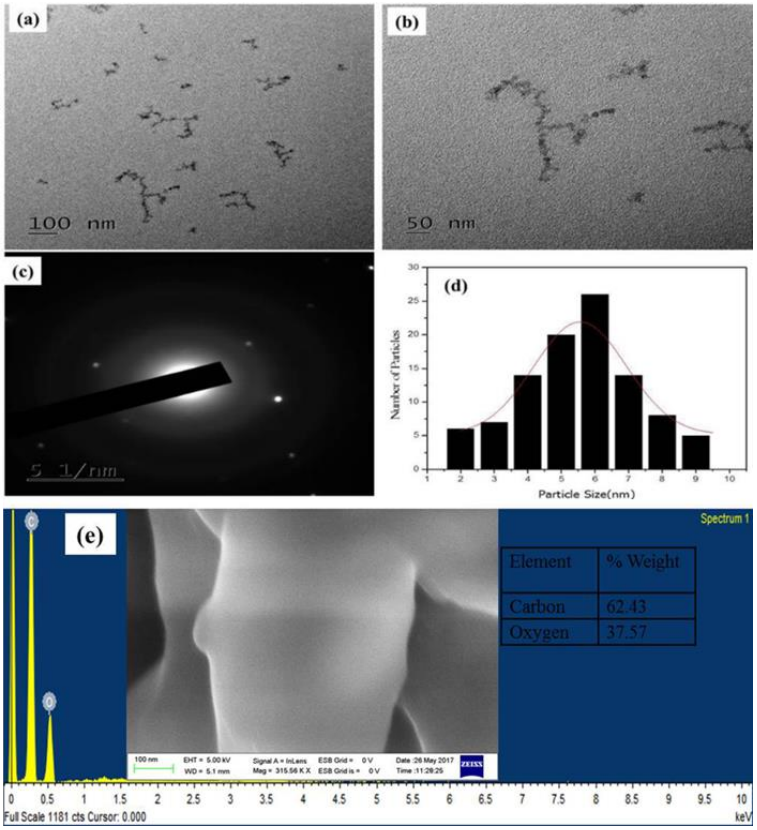

Fig 1. (a and b) TEM images, (c) SAED, (d) Particle size distribution histogram and (e) EDS spectrum insets are FESEM image and elemental composition of CQDs

Asian Journal of Nanoscience and Materials

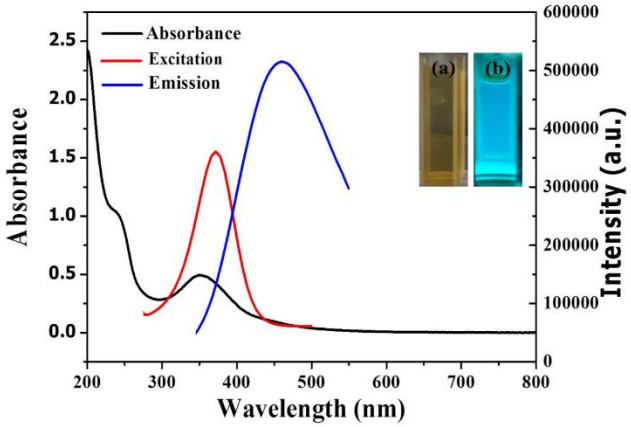

Fig 2. UV-Vis Absorption spectra of CQDs (black line), excitation (red line) and emission spectra (blue line); inset (a) CQDs solution under day light (b) under ultraviolet radiation

The photoluminescence properties depend up on concentration of CQDs. As shown in Fig 4a, symmetrical emission peaks observed at lower concentration and as concentration increase, the peaks split in to two indicating emission at two wavelength points with no variation in intensity of solution with different concentration. Ionic strength investigation using different concentration of sodium chloride (0.0383 M to 2 M NaCl) confirmed that varying concentration of salt has no significant effect on fluorescence of CQDs (Fig 4b). Changing pH of solution has effect on the fluorescence intensity of the CQDs but no effect on emission wavelength. As pH decrease from 6 to 2, the FL intensity increased (Fig 4d) and as pH increase from 6 to 12, the FL intensity decreased. Further, the CQDs have shown high photostability in that neither no shift in emission wavelength nor no significant reduction in FL intensity upon continuous exposure to ultraviolet radiation from 10 min to 24 h (Fig 4c) and 1 to 3 months preservation there is no change in fluorescence intensity.

Fourier transform infrared (FTIR) spectral investigation was undergone to describe about the functional groups present on the surface of CQDs. As seen in Fig 5a, there is a broad strong bands at 3300 cm^{-1} which can be assigned to the stretching vibration of the carboxylic O-H bonds. The band at 1070 cm^{-1} can be assigned to vibration of C-O bond. The appearances of bands at 2944 cm^{-1} indicate the presence of aliphatic C–H bond and the bands in range of 1040–1300 cm^{-1} illustrate the existence of C-O functional groups. The characteristic peaks at 1651 cm^{-1} and 1552 cm^{-1} indicate the presence of COO^- vibrational stretch. In addition, the existence of characteristic stretching vibrations for C=C in aromatic hydrocarbons at 1423 cm^{-1} confirms the presence of the aromatic skeleton in the prepared CQDs [15, 28–30]. Hence, the FTIR analysis shows the presence of important functional groups on the surface of lemon juice derived CQDs. The high water solubility of the CQDs is as a result of these different functional groups on the surface [31–33].

Asian Journal of Nanoscience and Materials

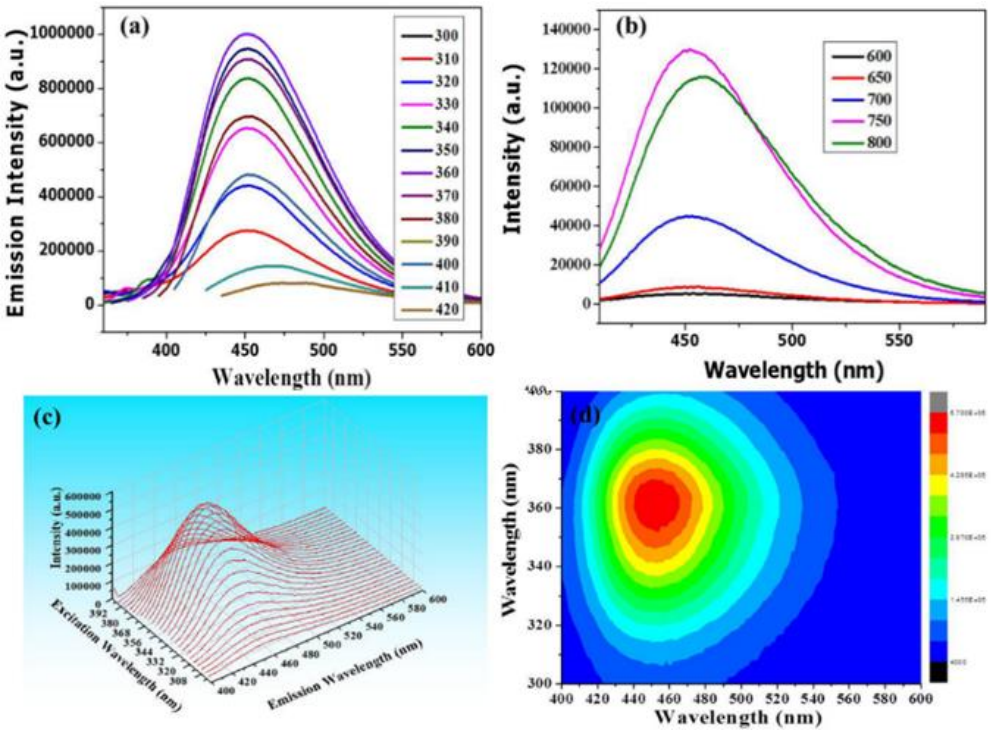

Fig 3. (a) PL emission spectra of CQDs at excitation wavelengths from 300 nm to 420 nm, (b) Upconverted PL emission spectra of CQDs at excitation wavelengths from 600 nm to 800 nm, (c) 3D Fluorescence Spectra of CQDs (Excitation with radiation from 300 nm to 400 nm and Corresponding Emission, (d) Excitation and emission contour map of CQDs.

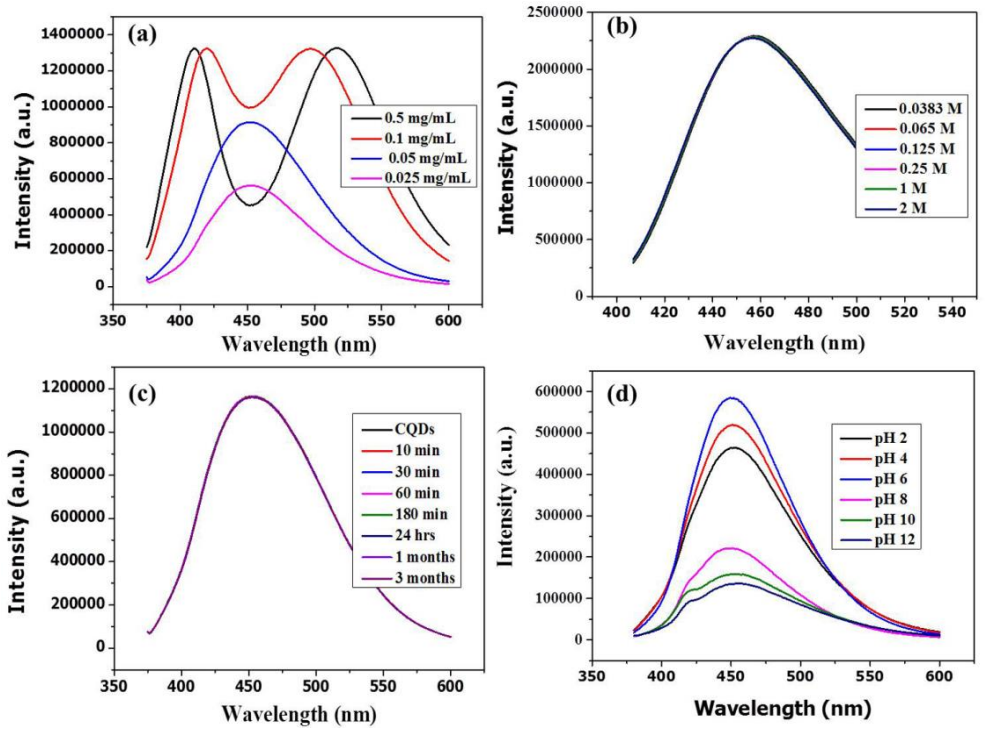

Fig 4. (a) Effect of concentration, (b) Effect of salt, (c) Effect of irradiation and preservation time, and (d) Effect of pH on photoluminescence of CQDs.

Asian Journal of Nanoscience and Materials

The XRD patterns show a broad and intense diffraction peak centered at $2\theta=23.5^0$ and weak peak at $2\theta=41^0$ which are assigned to (002) and (101) diffraction pattern of graphitic carbon as shown in Fig 5b which indicates the amorphous nature of the CQDs and is in accordance with previous structure analysis on disordered amorphous graphitic carbon quantum dots [34, 35]. The CQDs in aqueous solution were diluted for being deposited onto glass slide to have them individually dispersed for fluorescence imaging under single dot conditions. The fluorescence of the specimen could readily be detected under fluorescence microscopy, with the observed images confirming the uniform dispersion of the CQDs (Fig 5c and d).

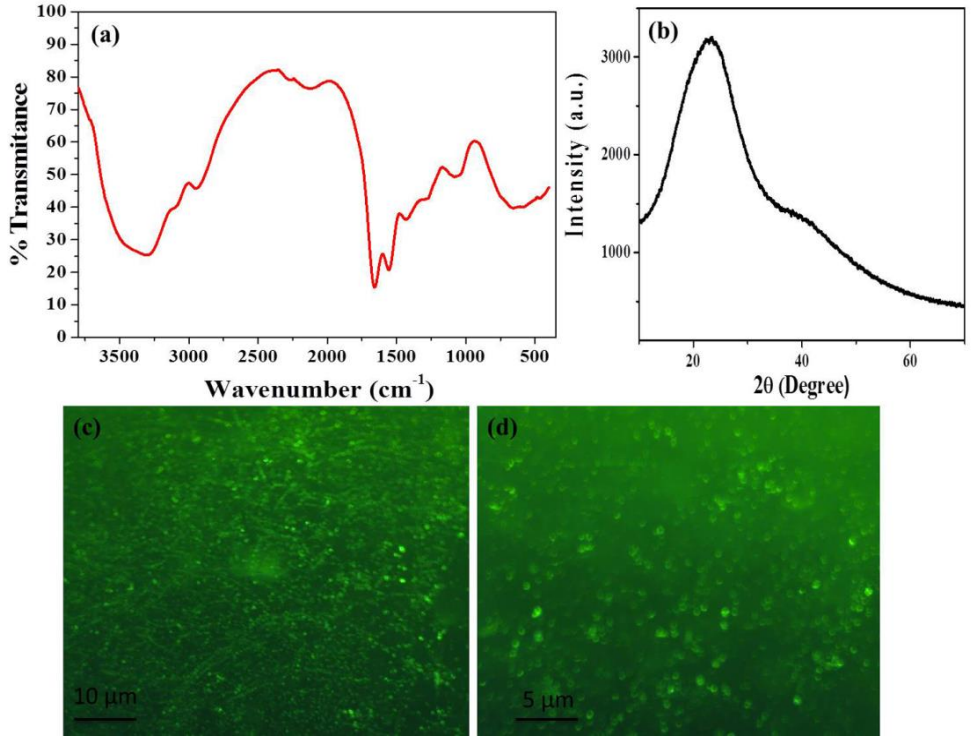

Fig 5. (a) FTIR spectra, (b) XRD and (c, d) fluorescence microscopic image of CQDs.

3.5 - Cell Cytotoxicity and Live Cell Imaging

The possible application of the as synthesized CQDs was evaluated for bioimaging of living cells. Cytotoxicity tendency of CQDs was evaluated in human breast adenocarcinoma (MCF7) cells through an MTT assay. Fig 6a shows that CQDs exhibited extremely low cytotoxicity with cell viability of about 85 % even at high concentration of 2 mg/mL and at 24 h of exposure time. The bright-field optical images also validated that there were no morphological change after the CQDs treatment, which suggested that the as-synthesized CQDs has good biocompatibility.

The bioimaging potential of the CQDs was evaluated by treating MCF7 cells with 0.025 mg/mL of lemon juice derived CQDs solution. After incubation for 4 h, the MCF7 were washed to remove extracellular CQDs and observed under fluorescent microscopy at laser excitations of 405, 488 and 561 nm. We found that the labelled cells were illuminated with multicolor images due to

fluorescence emitting from the CQDs distributed in the cell (Fig 6b-e) and exhibited blue, green and red fluorescence corresponding to the laser excitation at 405 nm, 488, nm and 561 nm. The results indicated that the highly water soluble, photostable fluorescent lemon juice derived carbon quantum dots can serve as an excellent fluorescence imaging probe.

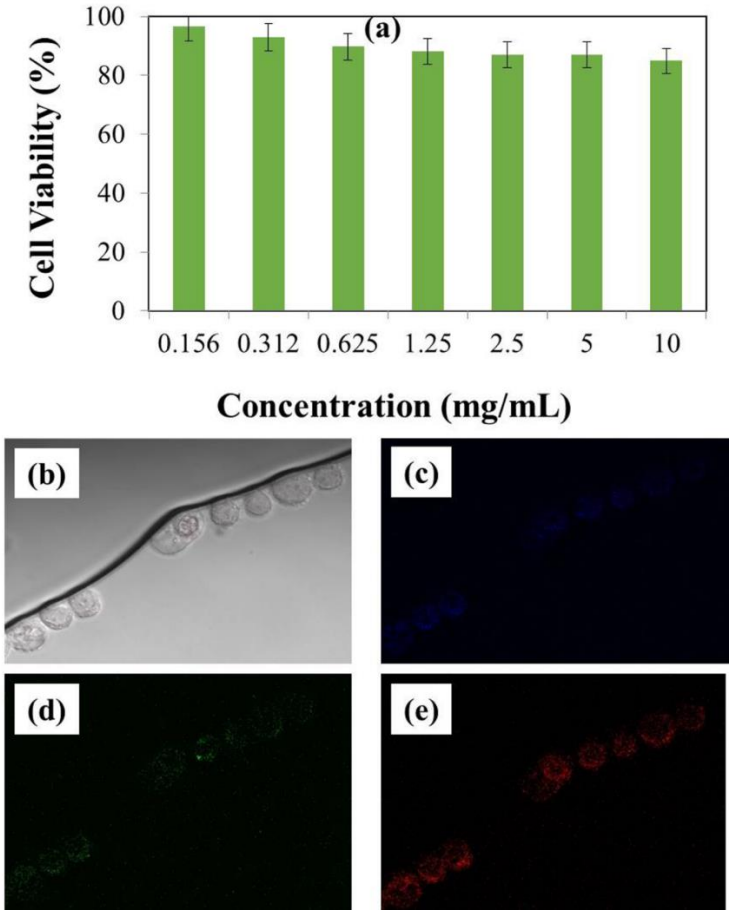

Fig 6. (a) Cell viability of MCF7 cells by MTT assay (b), (c), (d) and (e) confocal fluorescence microscopic images of CQDs labelled MCF7 cells under bright field, 405 nm excitation, 488 nm excitation and 561 nm excitation, respectively.

4 - Conclusions

We have successfully synthesized the CQDs from citrus lemon juice using simple green one pot hydrothermal method. The synthesized highly water soluble CQDs have bright photoluminescence with high stability to ionic solution and resistant to photobleaching. The fluorescence intensity of CQDs depends on the concentration and pH of the solution while emission wavelengths are not affected by pH. The synthesized CQDs revealed excellent biocompatibility and can be used as potential fluorescent probe in live cell imaging.

References:

1. X. Xu, R. Ray, Y. Gu, H. J. Ploehn, L. Gearheart, K. Raker and W. A. Scrivens (**2004**) J. *Am. Chem. Soc*. 126: 12736–12737.

2. Y.-P. Sun, B. Zhou, Y. Lin, W. Wang, K. A. Shiral Fernando, P. Pathak, M. J. Meziani, B. A. Harruff, X. Wang, H. Wang, P. G. Luo, H. Yang, M. E. Kose, B. Chen, L.

Monica Veca and S.-Y. Xie (**2006**) *J. Am. Chem. Soc*. 128: 7756–7757.
3. S. Zhu, Y. Song, X. Zhao, J. Shao, J. Zhang and B. Yang (**2015**) *Nano Res*. 8: 355–381.
4. Q. Liang, W. Ma, Y. Shi, Z. Li and X. Yang (**2013**) *Carbon*. 60: 421–428.
5. J. Zhou, X. Shan, J. Ma, Y. Gu, Z. Qian, J. Chen and H. Feng (**2014***) RSC Adv*. 4: 5465.
6. H. Yukawa, R. Tsukamoto, A. Kano, Y. Okamoto, M. Tokeshi, T. Ishikawa, M. Mizuno, and Y. Baba (**2013**) *J. Cell Sci. Ther*. 43:1
7. H. Ding, L.-W. Cheng, Y.-Y. Ma, J.-L. Kong and H.-M. Xiong (**2013**) *New J. Chem*. 37: 2515.
8. X. Yang, Y. Wang, X. Shen, C. Su, J. Yang, M. Piao, F. Jia, G. Gao, L. Zhang and Q. Lin (**2017**) *J. Colloid Interface Sci.* 492: 1–7.
9. L. Cao, S.-T. Yang, X. Wang, P. G. Luo, J.-H. Liu, S. Sahu, Y. Liu and Y.-P. Sun (**2012**) *Theranostics* 2: 295–301.
10. F. Wu, H. Su, K. Wang, W.-K. Wong and X. Zhu (**2017**) *Int. J. Nanomedicine* 12: 7375–7391.
11. T. N. J. I. Edison, R. Atchudan, M. G. Sethuraman, J.-J. Shim and Y. R. Lee (**2016**) *J. Photochem. Photobiol.* B 161: 154–161.
12. J. Wei and J. Qiu (**2014**) *Adv. Eng. Mater*. 17: 138–142.
13. R. Jelinek (**2016**) Carbon Quantum Dots: Synthesis, Properties and Applications, Springer.
14. H. M. R. Gonçalves, A. J. Duarte and J. C. G. Esteves da Silva (**2010**) Biosens. Bioelectron. 26: 1302–1306.
15. Z. Yan, J. Shu, Y. Yu, Z. Zhang, Z. Liu and J. Chen (**2015**) *Luminescence* 30: 388–392.
16. D. Kumar, K. Singh, V. Verma and H. S. Bhatti (**2014**) Journal of Bionanoscience 8: 274–279.
17. A. Sachdev and P. Gopinath (**2015**) Analyst 140: 4260–4269.
18. A. Prasannan and T. Imae (**2013***) Ind. Eng. Chem. Res*. 52: 15673–15678.
19. Y. Dong, J. Shao, C. Chen, H. Li, R. Wang, Y. Chi, X. Lin and G. Chen (**2012**) *Carbon* 50: 4738–4743.
20. S. Lu, S. Guo, P. Xu, X. Li, Y. Zhao, W. Gu and M. Xue (**2016**) *Int. J. Nanomedicine*. 11: 6325–6336.
21. A. Rauf, G. Uddin and J. Ali (**2014**) *Org. Med. Chem. Lett*. 4: 5.
22. K. L. Penniston, S. Y. Nakada, R. P. Holmes and D. G. Assimos (**2008**) *J. Endourol*. 22: 567–570.
23. D. Magde, G. E. Rojas and P. G. Seybold (**1999**) Photochem. Photobiol. 70: 737.
24. Z. S. Qian, L. J. Chai, Y. Y. Huang, C. Tang, J. J. Shen, J. R. Chen and H. Feng (**2015**) *Biosens. Bioelectron*. 68: 675–680.
25. A. B. Bourlinos, A. Stassinopoulos, D. Anglos, R. Zboril, M. Karakassides and E. P. Giannelis (**2008**) *Small* 4: 455–458.
26. K. A. S. Fernando, S. Sahu, Y. Liu, W. K. Lewis, E. A. Guliants, A. Jafariyan, P. Wang, C. E. Bunker and Y.-P. Sun (**2015**) *ACS Appl. Mater. Interfaces* 7: 8363–8376.
27. S. N. Baker and G. A. Baker (**2010**) *Angew. Chem. Int.* Ed Engl. 49: 6726–6744.
28. Y. Shi, Y. Pan, H. Zhang, Z. Zhang, M.-J. Li, C. Yi and M. Yang (**2014**) *Biosens. Bioelectron*. 56: 39–45.
29. P. Liu, C. Zhang, X. Liu and P. Cui (**2016**) *Appl. Surf. Sci*. 368: 122–128.
30. K. Dimos (2016*) Curr. Org. Chem*. 20: 682–695.

Asian Journal of Nanoscience and Materials

31. Q.-Y. Cai, J. Li, J. Ge, L. Zhang, Y.-L. Hu, Z.-H. Li and L.-B. Qu (**2015**) *Biosensors and Bioelectronics* 72: 31–36.
32. L. Tian, D. Ghosh, W. Chen, S. Pradhan, X. Chang and S. Chen (**2009**) *Chem. Mater*. 21: 2803–2809.
33. S. Zhu, X. Zhao, Y. Song, S. Lu and B. Yang (**2016**) *Nano Today* 11: 128–132.
34. A. Hao, X. Guo, Q. Wu, Y. Sun, C. Cong and W. Liu (**2016**) *J. Lumin*. 170: 90–96.
35. R. Jelinek (**2016**) Carbon Nanostructures 29–46.

How to cite this manuscript: Aschalew Tadesse, Dharmasoth Rama Devi, Mebrahtu Hagos, GangaRao Battu, Keloth Basavaiah. Facile green synthesis of fluorescent carbon quantum dotsfrom citrus lemon juice for live cell imaging.Asian Journal of Nanoscience and Materials, 2018, 1, 36-46.